Heat capacity study of magnetoelectronic phase separation in $La_{1-x}Sr_xCoO_3$ single crystals

C. He,[1] S. Eisenberg,[1] C. Jan,[1] H. Zheng,[2] J. F. Mitchell,[2] and C. Leighton[1,*]
[1]*Department of Chemical Engineering and Materials Science, University of Minnesota, Minneapolis, Minnesota 55455, USA*
[2]*Materials Science Division, Argonne National Laboratory, Argonne, Illinois 60439, USA*
(Received 21 May 2009; revised manuscript received 9 November 2009; published 11 December 2009)

We present a detailed investigation of the specific heat ($0.35<T<270$ K) and ordinary Hall effect (300 K) in $La_{1-x}Sr_xCoO_3$ single crystals at 11 doping values in the range $0.00<x<0.30$. The data reveal a considerable amount of information on the nature of the percolation transition, the crystal and electronic structures, and, most significantly, the magnetoelectronic phase inhomogeneity that has attracted such attention in this material. The observations include a discontinuity in Debye temperature accompanying the insulator-metal transition, direct evidence for the percolative nature of this transition, and a large electron mass enhancement in the metallic state, likely due to strong electron correlation effects. The various contributions to the heat capacity are shown to provide a detailed picture of the phase-separated state and its evolution with doping and are discussed in light of prior neutron-scattering and heat capacity data. This doping dependence provides strong evidence that the phase separation is restricted to a well-defined doping range, $0.04<x<0.22$, in agreement with a recently proposed model.

DOI: 10.1103/PhysRevB.80.214411 PACS number(s): 75.40.Cx, 75.47.Gk, 71.30.+h

I. INTRODUCTION

Due to its observation in a large number of materials (e.g., manganites and cuprates), and the key role that it plays in some of their most attractive properties (e.g., colossal magnetoresistance[1–3] and high-temperature superconductivity[4]), magnetoelectronic phase separation (MEPS), is an active research area in complex oxides.[5,6] This phenomenon refers to the spatial coexistence of multiple electronic and magnetic phases in a single specimen and has been observed in a variety of transition-metal oxides. The doped perovskite cobaltites, in particular, the large bandwidth $La_{1-x}Sr_xCoO_3$ (LSCO) system, have proven particularly well suited to fundamental studies of this magnetic phase separation effect. A large body of knowledge has been accumulated on LSCO, both with direct probes of the magnetic inhomogeneity such as neutron diffraction (ND),[7] nuclear magnetic resonance (NMR),[8–11] small-angle neutron scattering (SANS),[12–14] and inelastic neutron spectroscopy (INS),[15–17] as well as bulk probes such as magnetometry,[18–23] magnetotransport,[13,19,23–25] etc. The consensus from these studies is that at low doping (i.e., $x<0.15$) this system phase separates into nanoscopic (i.e., 1–3 nm) hole-rich droplets, or clusters, with strong ferromagnetic (FM) intracluster correlations, embedded in a hole-poor non-FM matrix.[13–16] The FM exchange interactions within the clusters are ascribed to Co^{3+}/Co^{4+} double exchange, and the system exhibits a magnetic freezing transition conceptually similar to superparamagnetic nanoparticles.[26] With increasing x the mean cluster diameter increases,[16,27] leading to a metal-insulator transition (MIT), which is thought to be of percolation type,[26] and a coincident crossover from short- to long-range FM at a critical doping value, $x_C=0.17-0.18$.[13,16,26] The Curie temperature (T_C) in the FM phase reaches about 225 K at $x=0.30$.[19] The large tolerance factor and small cation radius variance in the LSCO system results in relatively small distortions from cubic (the symmetry is rhombohedral, space group $R\bar{3}c$) which decrease with increasing doping, eventually vanishing around $x=0.5$.[18,19] This rhombohedral space group is incompatible with a static, long-range Jahn-Teller distortion, but short-range distortions have been reported in the (thermally excited) Jahn-Teller active spin state,[15,16] demonstrating a rich interplay between the lattice, magnetic, and spin-state degrees of freedom.

Study of MEPS using LSCO single crystals has been particularly instructive. The availability of high-quality crystals has enabled detailed inelastic neutron spectroscopy studies, which provide measurements of the cluster diameter via elastic peak widths,[16] and have revealed the incommensurate nature of the magnetism in the non-FM matrix.[17] Single crystals also provide access to intrinsic transport and magnetotransport properties,[13] which have provided vital information on the nature of the MIT, and the consequences of formation of the clustered state at low x.[13,26,28] Although the LSCO system has been studied intensively by numerous techniques (e.g., ND,[7] NMR,[8–11] SANS,[12–14] INS,[15–17] magnetometry,[18–23] transport and magnetotransport,[13,18,19,23–25] ac susceptibility,[7,19–21] thermopower,[18,29] etc.), many of which have been applied to single crystals, specific heat (C_P) is a bulk probe that has been studied in less detail, particularly for crystals. Despite the fact that heat capacity provides vital direct information on lattice dynamics, conduction electrons, magnetism, etc., (as aptly demonstrated by the work on the manganites[1–3,6,30]), it has been studied only sporadically in the cobaltites. Undoped polycrystalline $LaCoO_3$ was studied via heat capacity[31–33] to probe the well-known spin-state transition. This is associated with thermal excitation of Co^{3+} from low spin ($t_{2g}^6e_g^0$, $S=0$) states to finite spin states (i.e., $t_{2g}^5e_g^1$; $S=1$, or $t_{2g}^4e_g^2$, $S=2$)[34] across the small "spin gap" arising from the comparable magnitude of the crystal-field splitting and Hund's rule exchange energy, the details remaining highly controversial. Scattered reports at specific doping values of $Ln_{1-x}AE_xCoO_3$ (Ln=lanthanide, AE=Sr or Ca) compounds have appeared,[35–37] but systematic heat capacity work on $La_{1-x}Sr_xCoO_3$ is limited, and, to the best of

our knowledge, restricted to polycrystalline samples.[38,39] Detailed studies on the highest quality single crystals available are advantageous in terms of unambiguously determining intrinsic magnetic phase separation effects, particularly given the evidence of extrinsic chemical segregation effects in polycrystals at low processing temperatures[40,41]

In the current paper we provide a detailed and systematic study of the specific heat of LSCO single crystals over a wide temperature ($0.35<T<270$ K) and magnetic field range (up to 9 T), at a total of 11 doping values ($0.00<x<0.30$). Some aspects of this data were briefly discussed in Ref. 27, focusing solely on magnetic phase separation. In the current paper we provide a full description of the data and subsequent analysis. This comprehensive analysis of the data provides a considerable amount of information, including a discontinuity in Debye temperature across the zero-temperature metal-insulator transition, direct evidence of the percolation nature of this transition (from comparisons between the conductivity and the electronic specific heat), and a large electron-mass enhancement in the metallic state. The various contributions to $C_P(T)$ are tracked with x, and, in conjunction with recently reported neutron-scattering data, provide a detailed picture of the evolution of the phase-separated state with doping. The data provide additional evidence for the surprising result that the MEPS in LSCO is confined solely to a well-defined doping range ($0.04<x<0.22$). This observation is consistent with recent SANS,[27] heat capacity,[27] magnetotransport,[27] and NMR studies,[42] the agreement between multiple complementary techniques being particularly convincing. The significance of this result is that it can be used as evidence for a doping fluctuation mechanism for the magnetoelectronic inhomogeneity,[27] and is therefore important in terms of establishing the fundamental origin of the effect.

II. EXPERIMENTAL DETAILS

Single-crystal LSCO samples[43] were grown by floating zone methods and characterized structurally by x-ray and neutron diffractions, and chemically by atomic-absorption inductively coupled plasma spectroscopy and thermogravimetric analysis. The compositions studied are $x=0.00$, 0.05, 0.10, 0.15, 0.17, 0.18, 0.19, 0.20, 0.22, 0.25, and 0.30, i.e., they are grouped around the critical doping value of $x_C=0.17-0.18$. Heat capacity measurements in the 1.8–270 K range (up to 9 T) were made in a standard Quantum Design system using the relaxation method. All data are shown in units of joule per kelvin per mole of LSCO. The temperature range was extended to 0.35 K in a closed-cycle He^3 system. Ordinary Hall-effect measurements were made in fields to 9 T using ac excitation at 13.7 Hz on standard Hall-bar-type samples at 300 K. The anomalous Hall effect provides an additional contribution, even at $T>T_C$, but we have verified that 300 K is sufficiently in excess of T_C that this effect is minor, even for the high x samples.

III. RESULTS AND DISCUSSION

The global temperature dependence ($1.8<T<270$ K) of the zero magnetic field C_P is shown in Fig. 1 for all 11 doping values studied. The overall shape of $C_P(T)$ is as expected, and is generally consistent with prior work (e.g., Ref. 39). The high-T limiting value is consistent with the classical value of $3R$ per atomic site in the formula unit, where R is the molar gas constant. The most notable high-T feature is the clear "lambda anomaly" at T_C for the higher dopings, as expected for long-range ordered FMs.[44,45] Surprisingly, a noticeable feature is found *only* for $x=0.30$, 0.25, and 0.22 samples. $x=0.20$, 0.19, and 0.18 samples show no large anomaly at the ordering temperature[46] despite the fact that they exceed the critical doping for long-range FM order ($x_C=0.17-0.18$), and apparently exhibit a well-defined T_C in bulk magnetometry.[26] Figure 2(a) shows a "closeup" of the region $100<T<275$ K for $x=0.30$, 0.25, and 0.22, illustrating that the C_P anomaly becomes progressively weaker as x decreases, eventually becoming very small[46] at $x<0.22$. This is seen more clearly by subtracting a smooth background (excluding the region around T_C) using a third-order polynomial, to extract the excess magnetic heat capacity, $\Delta C_P(T)$, as shown in Fig. 2(b). The systematic decrease in magnitude with decreasing x is evident from this plot and can be quantified by calculating the magnetic entropy associated with the FM ordering transition,

$$S_{Mag}=\int_{T_1}^{T_2}\frac{\Delta C_P}{T}dT, \tag{1}$$

where T_1 and T_2 define a temperature interval straddling T_C, e.g., 125–275 K [see Fig. 2(b)]. Such an analysis results in $S_{Mag}=0.60$, 0.59, and 0.52 J mol^{-1} K^{-1} at $x=0.30$, 0.25, and 0.22, respectively, all of which are well below the expected full spin entropy of $R\ln(2S+1)$, where S is the spin of the Co ion. This point will be returned to below. Figure 2(b) also shows that the anomaly associated with the FM ordering broadens, and becomes more symmetric in shape, as x is decreased. At $x=0.30$ the anomaly has the characteristic lambda shape associated with a conventional second-order FM to paramagnetic phase transition, while at lower x it evolves into an almost symmetric peak. The full width at half maximum of the peak correspondingly increases from 20.1 K at $x=0.30$ to 29.7 K at $x=0.22$.

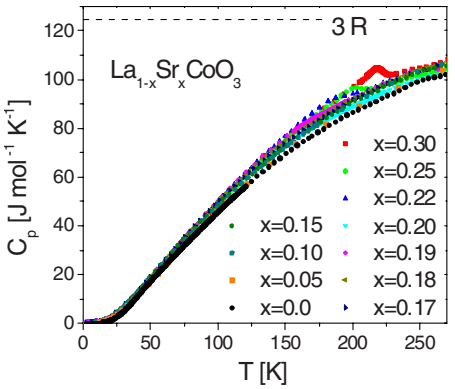

FIG. 1. (Color online) Temperature dependence of the zero-field specific heat ($1.8<T<270$ K) of 11 $La_{1-x}Sr_xCoO_3$ single crystals with $0.00<x<0.30$. The horizontal dashed line indicates the value of $3R$ per atom.

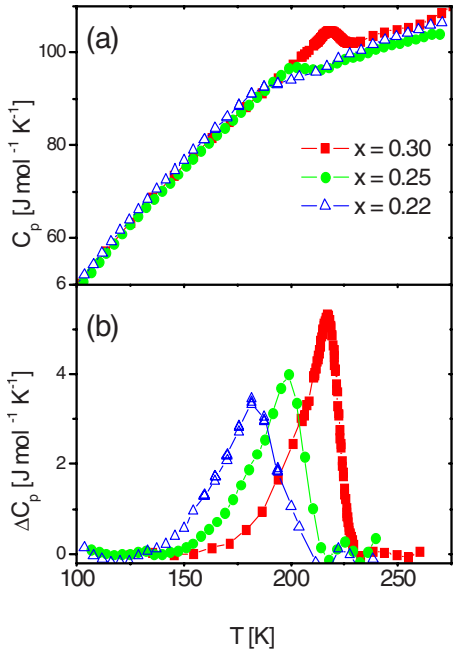

FIG. 2. (Color online) (a) Expanded view of the temperature dependence of the specific heat (Fig. 1) for $x=0.22$, 0.25, and 0.30 single crystals (i.e., those that exhibit clear anomalies at T_C). (b) Excess (magnetic) specific heat extracted from the data in (a) by subtracting a smooth background as described in the text.

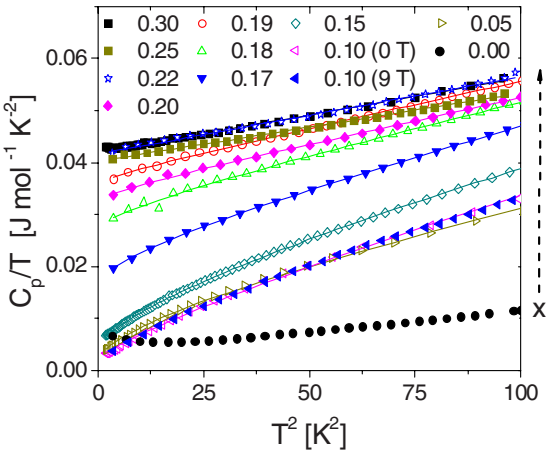

FIG. 3. (Color online) Temperature dependence of the specific heat ($1.8<T<10$ K) of 11 $La_{1-x}Sr_xCoO_3$ single crystals plotted as C_P/T vs T^2. The solid lines are fits to $C_P(T)=\gamma T+BT^2+\beta T^3$, a model that is described in detail in the text. The resulting parameters are plotted as a function of doping in Fig. 4. Some data are reproduced from (Ref. 27) with the permission of the publisher.

These observations from Figs. 1 and 2 clearly reveal two regimes of behavior separated by a critical doping value of $x=0.22$. Samples with $x \gg 0.22$ exhibit a large C_P anomaly at T_C with the classical lambda form, and a sharp well-defined critical scattering peak in SANS,[27] i.e., they exhibit features associated with conventional FMs. At $x=0.22$ we observe a smaller, broader, feature in both C_P and SANS,[27] while at $x<0.22$ the anomaly in C_P is very weak.[46] As discussed in more detail below, and in agreement with our recent SANS analysis,[27] we believe that these data indicate that $x=0.22$ marks an upper limit for the magnetoelectronic phase separation in LSCO, i.e., a phase-pure FM state exists at $x \geq 0.22$. Samples with $x \geq 0.22$ thus exhibit a clear lambda anomaly, although the spin entropy removed through the ordering transition is reduced in comparison to the expected value due to preformation of FM clusters as observed in our prior SANS work.[14] In the interval $0.18<x<0.22$ long-range FM order certainly exists [the magnetic correlation length is still observed to diverge as $T \rightarrow T_C^+$ (Ref. 27)] but the FM phase fraction is below 100%, i.e., MEPS is active and the system forms a percolated FM network in a non-FM (isolated cluster containing) background. This picture explains both the decrease in the magnitude of the peak value of ΔC_P and the peak width as x is decreased. When the FM phase fraction is less than one, coexistence of the long-range order in the percolated FM network with short-range order in the isolated FM clusters naturally leads to a broad distribution of local ordering/freezing temperatures, resulting in weaker, broader, features in $C_P(T)$. This is also consistent with the broad distribution in local internal hyperfine fields in recent NMR investigations.[42] We will see below that analysis of the low-T specific heat provides further evidence for an upper limit for the phase-separated regime at $x=0.22$, as discussed in Ref. 27.

The lower T region ($1.8<T<10$ K) is shown in more detail in Fig. 3 for all 11 samples measured. A subset of these data were originally discussed in Ref. 27, which focused solely on magnetic phase separation. The current paper provides a complete treatment of all of the data, including a full discussion of each of the identifiable contributions to the specific heat. The data are plotted as C_P/T vs T^2, as is commonly done to first test for a temperature dependence of the form,

$$C_P(T) = \gamma T + \beta T^3, \tag{2}$$

i.e., only electronic (γT) and lattice (βT^3) contributions to C_P. The electronic contribution, γ, is given in a free-electron model by $\gamma=\pi^2 k_B^2 N(E_F)/3$, where $N(E_F)$ is the density of states at the Fermi level, and the lattice contribution, β, is given in the Debye model by $\beta=234Nk_B/\Theta_D^3$, where N is the number of ions/mole and Θ_D is the Debye temperature. It is clear from Fig. 3 that at $x=0.30$, i.e., deep in the FM metallic state, Eq. (2) is indeed a good description of the data. We found that addition of a T^5 term to the lattice part of $C_P(T)$ was not required to achieve an adequate fit. [Note that the highest temperature used in this analysis (10 K) is a factor of 40–50 below Θ_D]. The observed intercept (i.e., γ) is very large, as will be discussed in detail below. This situation changes rapidly as x is decreased. The electronic contribution decreases as x decreases, as expected due to the approach to the metal-insulator transition, but this is accompanied by increasingly obvious systematic deviations from Eq. (2). In fact, it can be seen from Fig. 3 that the data deviate downwards from simple linear behavior on the C_P/T vs T^2 plot, suggesting an additional contribution to $C_P(T)$ with a T dependence weaker than T^3. This feature is, in fact, visible in previously published data on polycrystals but was not discussed in detail.[38,39] As the simplest possible means to quan-

tify this additional contribution we attempted to fit the data by adding a single power law term to Eq. (2), i.e., we added a term of the form CT^n, n (and C) being allowed to vary with x. This was found to provide a good fit to the data with $n = 2.10 \pm 0.16$ for x values of 0.05, 0.10, 0.15, and 0.17, suggestive that $n=2$, i.e., these data can be described with an additional BT^2 term in $C_P(T)$. The solid lines in Fig. 3 are thus fits to

$$C_P(T) = \gamma T + BT^2 + \beta T^3, \tag{3}$$

where B is a constant for a given doping value. This is found to describe the data very well for $0.05 < x < 0.30$. Before continuing to discuss the x dependence of the parameters γ, B, and β, and the origin of the BT^2 term, we should note that $C_P(T)$ at $x=0.00$ (the end member, $LaCoO_3$), is fundamentally different from all of the doped samples. For $x=0.00$, $C_P(T)/T$ shows an upturn at the lowest temperatures, as shown in Fig. 3. Measurements at still lower temperatures reveal that this is the high-T tail of a Schottky anomaly associated with the spin-state transition, an issue that was discussed in detail elsewhere.[47] As a final note on the data of Fig. 3 it is important to point out that an FM spin-wave contribution (often found to be of the form $T^{3/2}$) was not required to fit the data up to 10 K. We believe that this is consistent with the significant magnetocrystalline anisotropy in LSCO (Ref. 26) which should lead to a gapped spin-wave dispersion relation, and the likely absence of significant magnon excitation at such low T.

The doping dependence of the three contributions to $C_P(T)$, i.e., Θ_D, γ, and B, are shown in Figs. 4(a) and 4(c). Considering $\Theta_D(x)$ first, we see that the overall magnitude (380–500 K) is typical for perovskite oxides of this type and is in accord with measurements on comparable manganites such as $La_{1-x}Sr_xMnO_3$,[1,3,48,49] particularly single crystals.[1,49] The most surprising feature is the discontinuity in slope between $x=0.10$ and 0.15, suggesting a significant change in lattice dynamics around $x=0.125$. It is natural to correlate this with the known discontinuity in unit-cell parameters between $x=0.10$ and 0.15 (for both the lattice parameter, a, and rhombohedral angle, α), which was noticed as early as 1968 by Raccah and Goodenough.[50] The doping dependence of the room temperature unit-cell volume of the crystals studied in the current paper is shown in Fig. 4(b) for comparison to $\Theta_D(x)$, the discontinuity in the slope of $\Theta_D(x)$ clearly occurring at a similar x value to the discontinuity in cell volume. In light of the proximity to the critical doping value for the insulator-metal transition, and the crossover to true long-range FM order, Goodenough[50] interpreted the discontinuity in lattice parameters as evidence for coexistence of hole-rich FM metallic and hole-poor non-FM insulating regions, the two phases having distinct lattice parameters. We now know from direct measurements[8,13,16,17] that such magnetic phase separation does indeed take place, although the original interpretation in terms of gross segregation of Sr dopants is too literal. We mention parenthetically that the other obvious origin of such a lattice discontinuity would be the well-known spin-state transition of the Co^{3+} ion, which alters the t_{2g}/e_g orbital occupancy and hence the lattice parameters. However, at 300 K the Co^{3+} ions are already excited from the LS state

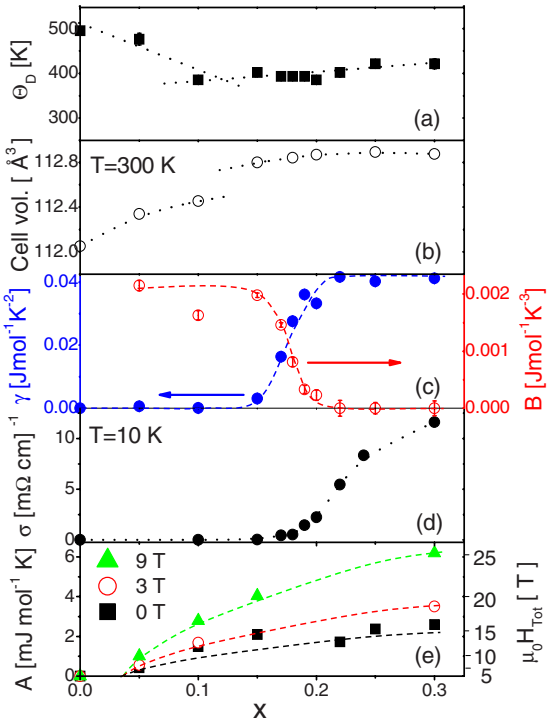

FIG. 4. (Color online) Doping dependence of (a) the Debye temperature, (b) the 300 K rhombohedral unit-cell volume (from x-ray diffraction), (c) the electronic (γ) and T^2 contributions (B) to the specific heat, (d) the 10 K conductivity, and (e) the nuclear contribution to the specific heat (A), at applied magnetic fields of 0, 3, and 9 T. Dashed lines are guides to the eyes. Error bars are shown in (a) and (c) but are similar in size to the data points. In (e) the error bars are also similar in size to the points. The right axis of (e) shows the conversion to hyperfine fields using the relation discussed in the text. Data in (c) and (e) are reproduced from Ref. 27 with the permission of the publisher.

to a finite spin state meaning that the spin-state transition is unlikely to dominate the room temperature x dependence of the cell volume. When the cell volume is examined as a function of doping at low T [e.g., 2 K (Ref. 7)] a large discontinuity *is* observed at low x (between $x=0.00$ and 0.10), consistent with the known stabilization of the finite spin states of the Co^{3+} ion with only light doping. Although it is tempting to suggest that it is the same lattice anomaly which gives rise to the discontinuities in Figs. 4(a) and 4(b), it is not clear how one then understands the details of the observed $\Theta_D(x)$. The $\Theta_D(x)$ we observe is, however, similar to that seen in $La_{1-x}Sr_xMnO_3$ single crystals,[1,49] where it was interpreted in terms of lattice softening induced by dynamical short-range Jahn-Teller distortions. Such distortions have also been implicated in LSCO (Refs. 15 and 16) and could well play the key role in determining $\Theta_D(x)$. Finally, although the correlation between Figs. 4(a) and 4(b) is quite convincing it should be mentioned that a small, low-T Schottky contribution to $C_P(T)$ [of the type present for $x=0.00$ (Ref. 47)], would provide additional specific heat at low T perhaps resulting in extraction of an erroneously high Θ_D and providing an alternative explanation for Fig. 4(a).

We now turn to the doping dependence of the electronic contribution as shown in Fig. 4(c) (left axis, solid points).

These data were discussed briefly in our earlier work[27] and are now discussed in detail, particularly with regards to the large magnitude of the electronic contribution and its relation to the conductivity. As expected, $\gamma \approx 0$ at low x (due to the nonmetallic nature of low doped LSCO), then increases near the MIT before abruptly saturating at $x=0.22$. The first point to be made about these data is that the saturation of γ at $x=0.22$ is further evidence for the onset of a phase pure FM metallic state at $x=0.22$ with essentially 100% FM phase fraction.[27] These data are therefore consistent with the analysis of the FM-ordering anomaly presented above (i.e., Figs. 1 and 2). We will see below that there exists even further evidence for the validity of this picture. The second noteworthy point about $\gamma(x)$ is that it provides further, very direct, evidence of the percolative nature of the MIT, which is expected in the phase-separation model.[19,26] This is seen clearly by comparing the doping dependence of the low-T conductivity [$\sigma(x)$,[26] Fig. 4(d)] with $\gamma(x)$. The more rapid increase in $\gamma(x)$ beyond the critical doping value results in a region near $x=0.18$ (i.e., just beyond x_C), where γ is high (67% of its saturation value) while the conductivity remains very low (only 4% of its value at $x=0.30$). Such a large electronic contribution to the specific heat in a system with low conductivity clearly argues for a spatially inhomogeneous charge-carrier distribution with hole-rich regions embedded in an insulating matrix, consistent with the accepted MEPS picture for LSCO.

The next point to discuss is the very large magnitude of γ at high x, i.e., in the region where we are dealing with a homogeneous phase-pure FM metallic state. Above $x=0.22$, γ reaches 41 mJ mol^{-1} K^{-2}, an order of magnitude larger than similar manganites, e.g., 3.5 mJ mol^{-1} K^{-2} in $x=0.30$ $La_{1-x}Sr_xMnO_3$ single crystals.[1,49] The observed γ in highly doped LSCO is in fact well within the range of what would typically be considered a heavy fermion system. It should be noted though that our value is quite consistent with other reports on polycrystalline LSCO which found $\gamma=41-43$ mJ mol^{-1} K^{-2} at $x=0.3$,[38,39] $\gamma=48$ mJ mol^{-1} K^{-2} at $x=0.33$,[35] and $\gamma=46$ mJ mol^{-1} K^{-2} at $x=1.0$,[51] as well as a solitary single-crystal measurement of 49 mJ mol^{-1} K^{-2} at $x=0.3$.[52] An important point to consider here is whether there is another contribution to $C_P(T)$ that is linear in T, i.e., whether γ could be composed of two contributions, one electronic, the other of some other origin, leading us to overestimate the electronic contribution. One obvious source of such an effect is magnetism. It is well known that spin glasses can exhibit a linear term in $C_P(T)$ and in fact it has been discussed in prior work on polycrystalline LSCO (Ref. 38) that this may be responsible for the large γ. The analysis presented above clearly suggests that for $x \geq 0.22$ (i.e., the region with the largest γ values) we have a phase-pure FM metallic state, strong evidence that we are *not* overestimating γ due to an additional spin-glass contribution. Neutron-scattering data demonstrate persistence of FM to low T in this region, with no suggestion of a re-entrant spin-glass phase. We would expect any glassy contribution to γ to show up in the low x region, where γ is, in fact, negligible. Another source of an additional linear contribution to $C_P(T)$ has been discussed in the context of nonstoichiometric $LaMnO_{3+\delta}$ materials,[53] which were found to have large γ values (up to 23 mJ mol^{-1} K^{-2}) even though they were electrically insulating. This effect was ascribed to a large density of *localized* states near E_F, the charge carriers being localized by magnetic or cationic disorder. This effect is not, however, a viable explanation for the anomalously large γ in LSCO. The full x dependence measured in the current manuscript [Fig. 4(c)] clearly shows no such effect at low x, i.e., γ is indeed zero when the system is insulating. All of this analysis argues that the γT contribution to $C_P(T)$ in LSCO is truly electronic in origin.

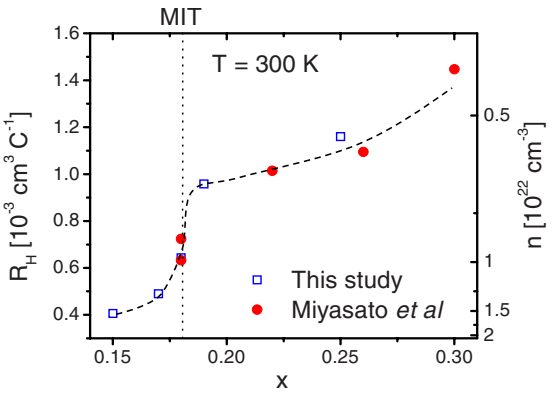

FIG. 5. (Color online) Doping dependence of the 300 K ordinary Hall coefficient of $La_{1-x}Sr_xCoO_3$ single crystals. Open squares are from this study and the solid circles are taken from Miyasato *et al.* (Ref. 52) The right axis shows the equivalent electron density, estimated from $n=1/R_He$. The dotted line is a guide to the eyes.

Applying the free-electron formula, $\gamma=\pi^2k_B^2N(E_F)/3$, we estimate $N(E_F) \approx 17.5$ states/eV/unit cell for $La_{0.7}Sr_{0.3}CoO_3$, which, although much larger than typical single-crystal manganites such as $La_{0.7}Sr_{0.3}MnO_3$ [where γ implies $N(E_F) \approx 1.4$ states/eV/unit cell],[1,49] is consistent with the low-T spin-lattice relaxation rate measured by NMR,[11] where the conduction electrons contribute via the orbital relaxation mechanism. First-principles electronic-structure calculations predict much smaller $N(E_F)$ for LSCO, however,[54] and $\gamma=7.5$ mJ mol^{-1} K^{-2}.[51] All of this indicates a significant mass enhancement. In order to further quantify this we performed room-temperature measurements of the ordinary Hall coefficient in order to directly estimate the charge-carrier density, which, when combined with the $N(E_F)$ from γ, provides an estimate of the effective mass, m^*. The x dependence of the 300 K ordinary Hall coefficient, R_H, is shown in Fig. 5, along with similar data from the work of Miyasato *et al.*[52] on LSCO single crystals.[55] Note that the sign of the Hall coefficient corresponds to hole conduction. The data reveal a striking change in character near the critical doping value for the insulator-metal transition. Below this value R_H is small and strongly x dependent, while above it, $R_H \approx 1.0-1.4\times10^{-3}$ cm^3 C^{-1}, weakly dependent on x and in reasonable agreement with prior work on manganites.[1,3] It is clear from these data that the ordinary Hall effect is suppressed below the percolation threshold, likely due to the known magnetoelectronic phase-separation effects, which result in strongly inhomogeneous conduction paths.[55–59] We believe that interpretation of the Hall data at low x will therefore require a detailed study of the interplay between the Hall

coefficient, the phase separation, and the inhomogeneous current distribution, which is beyond the scope of the current paper. Focusing on the high x region we see that the R_H values correspond to carrier densities, $n=1/R_He$ of $4-7\times10^{21}$ cm^{-3}, corresponding to ~0.3 holes per Co ion, in reasonable agreement with other perovskites at similar doping levels.[1,3] Using the free-electron relation between $N(E_F)$ and n, then gives $m^*=\hbar^2\pi^{4/3}N(E_F)/(3n)^{1/3}$, leading to $m^*\approx 43m_e$ for $x=0.3$. In agreement with the work of Balamurugan *et al.*[51] on $SrCoO_3$, we interpret this as being due to electron-correlation effects in the relatively narrow σ^* band, similar to $SrRuO_3$.[60] It should be noted that $\gamma(x)$ shows no evidence of an enhancement confined to the region near the insulator-metal transition in Fig. 4(c), indicating that we are not simply dealing with mass renormalization in the critical region, as often observed in doped Mott insulators.[1]

The final discussion point from Fig. 4 is the doping dependence of the T^2 term, i.e., $B(x)$, as shown in panel (c). This was discussed briefly in Ref. 27 but will now be covered in more detail, particularly with respect to the physical origin of this term. The most important insight into the origin of this contribution to $C_P(T)$ comes from the comparison between $B(x)$ and $\gamma(x)$. B remains high out to doping values approaching the MIT ($x\approx0.17$), beyond which it decreases smoothly to zero at $x=0.22$. It is clear from these data that $B(x)$ and $\gamma(x)$ exhibit what is essentially a reciprocal relationship, the obvious implication being that $B(x)$ is associated with the non-FM phase. What we observe in Fig. 4(c) is thus phase conversion from insulating non-FM to metallic FM with increasing x. Note that the signature of the non-FM phase (i.e., B) goes to zero at exactly $x=0.22$, the point at which the signature of the metallic FM phase (γ) saturates. As we have argued above this is the point where the magnetically phase-separated regime ends and a phase-pure FM metallic state is entered.

The physical mechanism in the non-FM phase giving rise to the T^2 contribution to $C_P(T)$ warrants further discussion. Such T^2 terms have been observed before in manganites, particularly undoped $LaMnO_3$.[48] $LaMnO_3$ is known from neutron diffraction to be an A-type antiferromagnet (AF) (i.e., sheets of FM spins coupled AF) and it was shown that a reasonable form for the spin-wave dispersion relation in such a spin structure does indeed lead to a T^2 contribution to $C_P(T)$,[48] and this was therefore taken as a plausible origin of this effect. This interpretation is not directly applicable to our case as undoped $LaCoO_3$ does not exhibit A type, or any other type, of AF order, and B remains finite even for $x>0$. However, at least at $x=0$, thermal excitation of simultaneous F and AF spin fluctuations has been observed in LSCO by INS,[16] a simple interpretation being the existence of A-type AF fluctuations.[16] It is possible that these fluctuations are the origin of the BT^2 term we observe. Although these fluctuations were detected only at $x=0$ in INS,[16] signal to noise issues could have obscured them in lightly doped samples. Cornelius *et al.*[61] also observed a T^2 contribution to $C_P(T)$ in electron-doped $CaMnO_3$. As an extension of the idea presented by Woodfield *et al.*[48] they interpreted the T^2 term as being due to long-wavelength excitations with both FM and AF components, due to the magnetic phase separation into nanometric FM droplets known to exist in that system.[62] This is very similar to our own situation and it is clear that additional theoretical work aimed at calculating $C_P(T)$ in systems of nanoscopic FM clusters in a non-FM matrix would be valuable. In terms of magnetism, the only other clear possibility would be the incommensurate behavior discovered by Phelan *et al.*[17] and interpreted in terms of seven-site magnetopolarons. Observations of similar polarons[63,64] or excitons[65,66] have been made at light doping by several groups and it is likely that such entities exist in the non-FM regions at higher x. It is clear that a theoretical study of the possible contribution of such magnetic entities to $C_P(T)$ is urgently required, but in the absence of such work we are unable to make definitive comments on the plausibility of this explanation. As a final comment we note that it is also possible that the T^2 term arises from some nonmagnetic feature of the non-FM phase. In fact, application of a 9 T magnetic field has little influence on $C_P(T)$ (see Fig. 3 where the $x=0.10$ data are shown both in zero field and 9 T as an example). This suggests that the BT^2 contribution is either nonmagnetic in origin or arises from a magnetic mechanism that is not significantly modified by a 9 T magnetic field. Fields of this order have been observed to induce some level of FM cluster coalescence, and an accompanying increase in FM phase fraction, but isolated clusters remain. This has been observed both in INS (Ref. 67) and SANS (Ref. 68) experiments. The absence of a strong field dependence does not therefore immediately rule out small clusters/polarons as the origin of the T^2 term. In any case, although the exact mechanism leading to the T^2 contribution to $C_P(T)$ remains unclear we can be definitive in ascribing it to the non-FM phase. The data of Fig. 4(c) therefore show that specific heat provides a very direct probe of the evolution of the MEPS with doping, an important conclusion being the clear indication of an upper limit for phase separation at $x=0.22$, in agreement with recent SANS data.[27]

Figure 6 shows that extending the T range of the measurement to 0.35 K provides considerable additional information. These data are again plotted as C_P/T vs T^2, using $x=0.05$, 0.10, 0.15, and 0.30 as representative compositions, although all samples with $x\geq0.05$ show such an effect. Applied magnetic fields of 0, 3, and 9 T are shown, over a temperature range from 0.35 to 1.5 K. Note that C_P increases with H at low T, a point which will be returned to later. The important feature in the data is the large increase in $C_P(T)$ at the lowest temperatures, a feature which is, in fact, common in magnetic materials and has been observed in manganites.[30,48,61,69] This was discussed briefly in Ref. 27 and is now discussed in detail. This feature is understood to be the high-T tail of a Schottky anomaly due to splitting of the nuclear-energy levels. This is observable at these relatively high temperatures in magnetically ordered materials due to the large values of internal magnetic field present. In essence, the internal magnetic fields, generated by the electron system, generate a nuclear-energy-level splitting, which results in a two energy-level system with $\Delta E=2\mu_{Nuc}H_{hf}$ (we have used a nuclear spin, $I=1/2$ for the purposes of simple illustration), where μ_{Nuc} is the nuclear moment and H_{hf} is the hyperfine field. The resulting two-level system leads to a nuclear Schottky contribution to the specific heat (C_P^{Nuc}) of the form,[70,71]

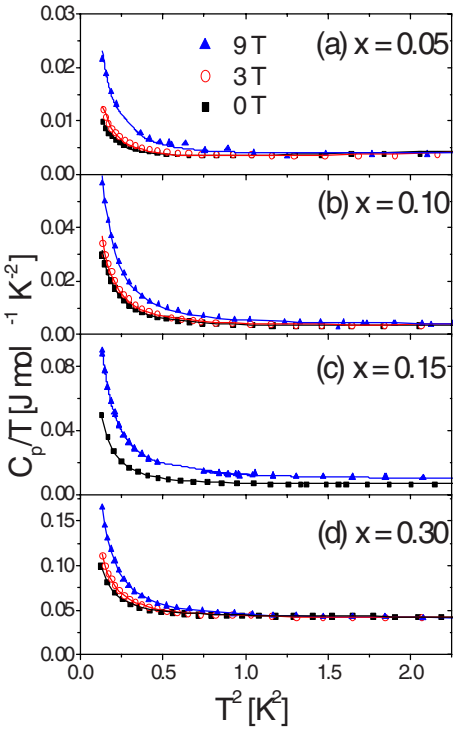

FIG. 6. (Color online) Temperature dependence of the specific heat ($0.35 < T < 1.5$ K) of (a) $x=0.05$, (b) $x=0.10$, (c) $x=0.15$, and (d) $x=0.30$ $La_{1-x}Sr_xCoO_3$ single crystals plotted as C_P/T vs T^2, in applied magnetic fields of 0, 3, and 9 T. The solid lines are fits to the model described in the text.

$$C_P^{Nuc} = R\left(\frac{\Delta E}{k_B T}\right)^2 \frac{g_0}{g_1} \frac{\exp(\Delta E/k_B T)}{\left[1+\left(\frac{g_0}{g_1}\right)\exp(\Delta E/k_B T)\right]^2}, \quad (4)$$

where g_0 and g_1 are the degeneracies of the lower and higher energy levels and ΔE is the energy gap between these two levels. This equation predicts a peak in $C_P(T)$ in the vicinity of 10 mK, meaning that the data of Fig. 6 are simply the high-T tail of this feature. In the limit $T \gg \Delta E$, Eq. (4) reduces to $C_P^{Nuc} \approx A/T^2$, where the constant A is related to H_{hf} by,[30,61,69,72]

$$A = \frac{R}{3}\left(\frac{I+1}{I}\right)\left(\frac{\mu_{Nuc} H_{hf}}{k_B}\right)^2. \quad (5)$$

Note that $I=7/2$ and $\mu_{Nuc}=4.64$ nuclear magnetons for ^{59}Co, and that H_{hf} is the hyperfine field at the Co site. The important point here is that the parameter A provides a direct measure of the local internal field, allowing us to probe the magnetic ordering as a function of x. Addition of this nuclear Schottky contribution to Eq. (3) results in

$$C_P(T) = \gamma T + BT^2 + \beta T^3 + \frac{A}{T^2}, \quad (6)$$

which generates the solid lines shown in Fig. 6, confirming that it is indeed a good description of the data. Note that although we now have four distinct contributions to $C_P(T)$, the final term in Eq. (6) is so dominant at low T (for example, it contributes about 96% of the heat capacity at 0.39 K for $x=0.10$), the parameter A can still be reliably determined.

The doping and magnetic field dependence of the H_{hf} values extracted from A [using Eq. (5)] are illustrated in Fig. 4(e). The field dependence rules out the possibility of paramagnetic impurities as the origin of this Schottky anomaly since in that case, application of magnetic fields on the order of 9 T should strongly suppress the heat capacity, exactly opposite to our observations. Previous zero-field NMR measurements probing the ^{59}Co nucleus revealed a broad peak centered at a frequency of approximately 172 MHz corresponding to an internal field of 17.1 T in the FM phase.[8] This is in good agreement with the value of H_{hf} of 15.9 T at $x=0.30$ [Fig. 4(e), right axis], demonstrating that at high x the data of Fig. 6 are quantitatively consistent with the known features of the long-range FM ordering. The intriguing aspect of the data in Fig. 4(e) is the behavior in the lower x region. Decreasing x from 0.30 results in a decrease in H_{hf} due to the weakening of the FM ordering, as expected, but we observe no clear feature at the critical doping value of $x=0.17-0.18$. Clearly this is due to the persistence of short-range FM ordering well below the critical composition, consistent with the general phase-separation picture. The surprising feature of the data is the apparent vanishing of H_{hf} at a well-defined doping value, estimated by extrapolation to be $x \approx 0.04$. This suggests that the short-range magnetic order from the FM clusters disappears abruptly at $x \approx 0.04$. We have already argued above that there exists a well-defined upper limit to the region over which phase separation occurs at $x \approx 0.22$, which is, in fact, qualitatively consistent with the theoretical work of Suzuki *et al.*[73] showing a crossover from a phase separated to homogeneous state at high doping. The data of Fig. 4(e) additionally suggest a *lower* limit of $x \approx 0.04$, defining an interval, $0.04 < x < 0.22$, over which MEPS is active, as pointed out in our earlier work.[27] Complementary SANS data on the same crystals also show a clear onset of high q scattering intensity around $x=0.04$,[27] further validation of this result. We recently used this unanticipated result that the phase separation is confined to a precise doping range as they key piece of evidence to argue that the phase separation is doping fluctuation driven rather than being true electronic phase separation.[27]

There are certain aspects to this observation of a well-defined range over which phase separation occurs which warrant further discussion. The first of these is the lower limit of $x=0.04$. A significant number of investigations, using techniques such as NMR,[42] INS,[64] muon spin relaxation,[65,66] and susceptibility[63] have concluded that local magnetic entities are certainly present below this limit. These local magnetic entities have been given a variety of labels such as "magnetopolarons,"[17] "spin polarons,"[42] "magnetic excitons,"[65,66] and "spin-state polarons"[64] but it is clear that they all describe magnetic inhomogeneity at low or zero doping. We do not believe that this is contradictory to the results presented in the current paper. It is our hypothesis that these entities are precursors[65,66] to the strongly FM-correlated clusters observed in SANS and heat capacity, which are apparently only present in large enough quantities to be detected by SANS above $x \approx 0.04$. It is not currently clear exactly

how the evolution from "polaron" to "cluster" takes place or exactly what the distinctions are between the two terms, although the presence, or otherwise, of magnetocrystalline anisotropy could play an important role. It could also be that the detection limits of the various experimental techniques is a factor that contributes significantly to this confusion, and this is obviously an area that would benefit from additional work. Another important point is that the range over which phase separation occurs in *polycrystalline* LSCO is distinctly larger than for single crystals. NMR studies suggest that the range in polycrystals could be as high as $0.00<x<0.50$,[8] significantly widened in comparison to the single crystals studied here. We believe that this is likely due to additional, extrinsic, Sr-doping inhomogeneity due to incomplete solid-state reaction. It has been observed in prior work that the signatures of magnetic phase separation weaken with increasing firing temperature in polycrystalline samples,[40,41] which fits with this picture. The single crystals, where the magnetic phase-separation limits can be understood within the picture of purely random Sr distributions,[27] are the ultimate limit of such studies.

IV. SUMMARY

In summary, we have performed a comprehensive study of heat capacity and ordinary Hall effect in $La_{1-x}Sr_xCoO_3$ single crystals ($0.00<x<0.30$). We observed three conventional contributions to the heat capacity at low T. A lattice contribution ($\propto T^3$), an electronic contribution ($\propto T$), and a nuclear contribution (A/T^2), in addition to an unexpected T^2 contribution which originates in the nonferromagnetic phase. The doping dependence of these terms was analyzed in detail, providing a significant amount of information. In particular, we found evidence for a softening of the lattice at intermediate doping values, strong additional evidence for the percolation nature of the insulator-metal transition, and a large electron mass enhancement due to strong electron-electron correlations in the ferromagnetic metallic state. Additionally, the doping dependence of the T^2 contribution, electronic contribution, and nuclear Schottky anomaly, when considered with prior neutron-scattering and specific-heat data, were shown to provide a detailed picture of the evolution of the phase-separated state with doping. These results not only clarify the systematics of the magnetic phase separation in the important $La_{1-x}Sr_xCoO_3$ system, they also reiterate the capabilities of specific-heat measurements as a powerful probe of magnetic inhomogeneity, particularly when performed as a function of doping.

ACKNOWLEDGMENTS

Work at UMN was supported by DOE (Grant No. DE-FG02-06ER46275) (specifically the neutron-scattering data), NSF (Grant No. DMR-0804432) and used shared facilities from the NSF MRSEC. We would like to thank M. Hoch (National High Field Magnetic Laboratory) and S. El-Khatib (UMN and NIST) for useful discussions.

*Corresponding author; leighton@umn.edu

[1] Y. Tokura and Y. Tomioka, J. Magn. Magn. Mater. **200**, 1 (1999).
[2] J. M. D. Coey, M. Viret, and S. von Molnár, Adv. Phys. **48**, 167 (1999).
[3] M. B. Salamon and M. Jaime, Rev. Mod. Phys. **73**, 583 (2001).
[4] P. A. Lee, N. Nagaosa, and W. Xiao-Gang, Rev. Mod. Phys. **78**, 17 (2006).
[5] For a review see, E. Dagotto, T. Hotta, and A. Moreo, Phys. Rep. **344**, 1 (2001).
[6] E. Dagotto, *Nanoscale Phase Separation and Colossal Magnetoresistance* (Springer, New York, 2002).
[7] R. Caciuffo, D. Rinaldi, G. Barucca, J. Mira, J. Rivas, M. A. Senaris-Rodriguez, P. G. Radaelli, D. Fiorani, and J. B. Goodenough, Phys. Rev. B **59**, 1068 (1999).
[8] P. L. Kuhns, M. J. R. Hoch, W. G. Moulton, A. P. Reyes, J. Wu, and C. Leighton, Phys. Rev. Lett. **91**, 127202 (2003).
[9] M. J. R. Hoch, P. L. Kuhns, W. G. Moulton, A. P. Reyes, J. Wu, and C. Leighton, Phys. Rev. B **69**, 014425 (2004).
[10] M. J. R. Hoch, P. L. Kuhns, W. G. Moulton, A. P. Reyes, J. Lu, J. Wu, and C. Leighton, Phys. Rev. B **70**, 174443 (2004).
[11] M. J. R. Hoch, P. L. Kuhns, W. G. Moulton, A. P. Reyes, M. A. Torija, J. F. Mitchell, and C. Leighton, Phys. Rev. B **75**, 104421 (2007).
[12] R. Caciuffo, J. Mira, J. Rivas, M. A. Senaris-Rodriguez, P. G. Radaelli, F. Carsughi, D. Fiorani, and J. B. Goodenough, Europhys. Lett. **45**, 399 (1999).
[13] J. Wu, J. W. Lynn, C. J. Glinka, J. Burley, H. Zheng, J. F. Mitchell, and C. Leighton, Phys. Rev. Lett. **94**, 037201 (2005).
[14] C. He, M. A. Torija, J. Wu, J. W. Lynn, H. Zheng, J. F. Mitchell, and C. Leighton, Phys. Rev. B **76**, 014401 (2007).
[15] D. Louca and J. L. Sarrao, Phys. Rev. Lett. **91**, 155501 (2003).
[16] D. Phelan, D. Louca, S. Rosenkranz, S.-H. Lee, Y. Qiu, P. J. Chupas, R. Osborn, H. Zheng, J. F. Mitchell, J. R. D. Copley, J. L. Sarrao, and Y. Moritomo, Phys. Rev. Lett. **96**, 027201 (2006).
[17] D. Phelan, D. Louca, K. Kamazawa, S.-H. Lee, S. Rosenkranz, M. F. Hundley, J. F. Mitchell, Y. Motome, S. N. Ancona, and Y. Moritomo, Phys. Rev. Lett. **97**, 235501 (2006).
[18] M. A. Señarís-Rodríguez and J. B. Goodenough, J. Solid State Chem. **118**, 323 (1995).
[19] J. Wu and C. Leighton, Phys. Rev. B **67**, 174408 (2003).
[20] D. N. H. Nam, K. Jonason, P. Nordblad, N. V. Khiem, and N. X. Phuc, Phys. Rev. B **59**, 4189 (1999).
[21] S. Mukherjee, R. Ranganathan, P. S. Anilkumar, and P. A. Joy, Phys. Rev. B **54**, 9267 (1996).
[22] I. Fita, R. Szymczak, R. Puzniak, I. O. Troyanchuk, J. Fink-Finowicki, Y. M. Mukovskii, V. N. Varyukhin, and H. Szymczak, Phys. Rev. B **71**, 214404 (2005).
[23] M. Kriener, C. Zobel, A. Reichl, J. Baier, M. Cwik, K. Berggold, H. Kierspel, O. Zabara, A. Freimuth, and T. Lorenz, Phys. Rev. B **69**, 094417 (2004).
[24] R. Mahendiran and A. K. Raychaudhuri, Phys. Rev. B **54**, 16044

(1996).
[25] V. Golovanov, L. Mihaly, and A. R. Moodenbaugh, Phys. Rev. B **53**, 8207 (1996).
[26] H. M. Aarbogh, J. Wu, L. Wang, H. Zheng, J. F. Mitchell, and C. Leighton, Phys. Rev. B **74**, 134408 (2006).
[27] C. He, S. El-Khatib, J. Wu, J. W. Lynn, H. Zheng, J. F. Mitchell, and C. Leighton, EPL **87**, 27006 (2009).
[28] J. Wu, H. Zheng, J. F. Mitchell, and C. Leighton, Phys. Rev. B. **73**, 020404(R) (2006).
[29] K. Berggold, M. Kriener, C. Zobel, A. Reichl, M. Reuther, R. Muller, A. Freimuth, and T. Lorenz, Phys. Rev. B **72**, 155116 (2005).
[30] J. J. Neumeier and A. L. Cornelius, in *Nanoscale Phase Separation and Colossal Magnetoresistance* by E. Dagotto (Springer, New York, 2002), p. 251.
[31] S. Stølen, F. Gronvold, H. Brinks, T. Atake, and H. Mori, Phys. Rev. B **55**, 14103 (1997).
[32] T. Kyômen, Y. Asaka, and M. Itoh, Phys. Rev. B **71**, 024418 (2005).
[33] M. Tachibana, T. Yoshida, H. Kawaji, T. Atake, and E. Takayama-Muromachi, Phys. Rev. B **77**, 094402 (2008).
[34] For a brief review see, M. Imada, A. Fujimori, and Y. Tokura, Rev. Mod. Phys. **70**, 1039 (1998).
[35] M. Paraskevopoulos, J. Hemberger, A. Krimmel, and A. Loidl, Phys. Rev. B **63**, 224416 (2001).
[36] R. Mahendiran and P. Schiffer, Phys. Rev. B **68**, 024427 (2003).
[37] S. Tsubouchi, T. Kyômen, M. Itoh, and M. Oguni, Phys. Rev. B **69**, 144406 (2004).
[38] K. Muta, Y. Kobayashi, and K. Asai, J. Phys. Soc. Jpn. **71**, 2784 (2002).
[39] S. Tsubouchi, T. Kyomen, and M. Itoh, Phys. Rev. B **67**, 094437 (2003).
[40] J. Mira, J. Rivas, G. Baio, G. Barucca, R. Caciuffo, D. Rinaldi, D. Fiorani, and M. A. Senaris Rodriguez, J. Appl. Phys. **89**, 5606 (2001).
[41] D. Samal, K. Balamurugan, C. Shivakumara, and P. S. Anil Kumar, J. Appl. Phys. **105**, 07E320 (2009).
[42] R. X. Smith, M. J. R. Hoch, P. L. Kuhns, W. G. Moulton, A. P. Reyes, G. S. Boebinger, J. Mitchell, and C. Leighton, Phys. Rev. B **78**, 092201 (2008).
[43] These are the same single crystals used in Refs. 13, 15–17, and 26–28.
[44] D. Kim, B. Revaz, B. L. Zink, F. Hellman, J. J. Rhyne, and J. F. Mitchell, Phys. Rev. Lett. **89**, 227202 (2002).
[45] J. E. Gordon, S. D. Bader, J. F. Mitchell, R. Osborn, and S. Rosenkranz, Phys. Rev. B **60**, 6258 (1999).
[46] Close analysis of the field-dependent part of $C_P(T)$ reveals weak features associated with the magnetic-ordering transitions all the way down to $x=0.10$ (Ref. 39). This does not alter our argument for a distinct difference in behavior between $x=0.20$ and 0.22.
[47] C. He, H. Zheng, J. F. Mitchell, M. L. Foo, R. J. Cava, and C. Leighton, Appl. Phys. Lett. **94**, 102514 (2009).
[48] B. F. Woodfield, M. L. Wilson, and J. M. Byers, Phys. Rev. Lett. **78**, 3201 (1997).
[49] T. Okuda, A. Asamitsu, Y. Tomioka, T. Kimura, Y. Taguchi, and Y. Tokura, Phys. Rev. Lett. **81**, 3203 (1998).
[50] P. M. Raccah and J. B. Goodenough, J. Appl. Phys. **39**, 1209 (1968).
[51] S. Balamurugan, K. Yamaura, A. B. Karki, D. P. Young, M. Arai, and E. Takayama-Muromachi, Phys. Rev. B **74**, 172406 (2006).
[52] T. Miyasato, N. Abe, T. Fujii, A. Asamitsu, S. Onoda, Y. Onose, N. Nagaosa, and Y. Tokura, Phys. Rev. Lett. **99**, 086602 (2007).
[53] L. Ghivelder, I. A. Castillo, M. A. Gusmao, J. A. Alonso, and L. F. Cohen, Phys. Rev. B **60**, 12184 (1999).
[54] P. Ravindran, H. Fjellvag, A. Kjekshus, P. Blaha, K. Scwarz, and J. Luitz, J. Appl. Phys. **91**, 291 (2002).
[55] Y. Onose and Y. Tokura, Phys. Rev. B **73**, 174421 (2006).
[56] V. Orlyanchik, M. B. Weissman, M. A. Torija, M. Sharma, and C. Leighton, Phys. Rev. B **78**, 094430 (2008).
[57] Similar effects have been suggested as the origin of an enhanced anomalous Hall coefficient in $La_{1-x}Ca_xCoO_3$ crystals and films (Refs. 58 and 59).
[58] S. A. Baily, M. B. Salamon, Y. Kobayashi, and K. Asai, Appl. Phys. Lett. **80**, 3138 (2002).
[59] A. V. Samoilov, G. Beach, C. C. Fu, N.-C. Yeh, and R. P. Vasquez, Phys. Rev. B **57**, R14032 (1998).
[60] J. Okamoto, T. Mizokawa, A. Fujimori, I. Hase, M. Nohara, H. Takagi, Y. Takeda, and M. Takano, Phys. Rev. B **60**, 2281 (1999).
[61] A. L. Cornelius, B. E. Light, and J. J. Neumeier, Phys. Rev. B **68**, 014403 (2003).
[62] E. Granado, C. D. Ling, J. J. Neumeier, J. W. Lynn, and D. N. Argyriou, Phys. Rev. B **68**, 134440 (2003).
[63] S. Yamaguchi, Y. Okimoto, H. Taniguchi, and Y. Tokura, Phys. Rev. B **53**, R2926 (1996).
[64] A. Podlesnyak, M. Russina, A. Furrer, A. Alfonsov, E. Vavilova, V. Kataev, B. Buchner, Th. Strassle, E. Pomjakushina, K. Conder, and D. I. Khomskii, Phys. Rev. Lett. **101**, 247603 (2008).
[65] S. R. Giblin, I. Terry, S. Clarke, T. Prokscha, A. T. Boothroyd, J. Wu, and C. Leighton, Europhys. Lett. **70**, 677 (2005).
[66] S. R. Giblin, I. Terry, D. Prabhakaran, A. T. Boothroyd, J. Wu, and C. Leighton, Phys. Rev. B **74**, 104411 (2006).
[67] D. Phelan, D. Louca, S. N. Ancona, S. Rosenkranz, H. Zheng, and J. F. Mitchell, Phys. Rev. B **79**, 094420 (2009).
[68] J. Wu, J. W. Lynn, and C. Leighton (unpublished).
[69] M. R. Lees, O. A. Petrenko, G. Balakrishnan, and D. McK. Paul, Phys. Rev. B **59**, 1298 (1999).
[70] E. S. R. Gopal, *Specific Heats at Low Temperatures* (Plenum, New York, 1966).
[71] H. M. Rosenberg, *Low Temperature Solid State Physics* (Oxford University Press, Oxford, 1963).
[72] H. Kopferman, *Nuclear Moments* (Academic, New York, 1958).
[73] R. Suzuki, T. Watanabe, and S. Ishihara, Phys. Rev. B **80**, 054410 (2009).